Journal of Engineering and Applied Sciences 11 (9): 2028-2035, 2016
ISSN: 1816-949X

Development of Micro Surface Topography Prediction Software for an End Mill

Dong-Hyeon Kim, Sang-Won Seo, De-Jun Cheng and Su-Jin Kim
Department of Mechanical Engineering, Gyeongsang National University,
52818 Jinju, Republic of Korea

Abstract: This study presents the development of software to predict the micro surface topography generated by an end mill. The software was developed using Visual C++ language. Milling experiments and other previous research results were used to validate the estimation capability of the software. A good agreement was found between reference data and prediction results. Furthermore, discrepancies between experimental and prediction results for the ball end mill were compensated by linear equations. Finally, the validated micro surface topography software can be used to predict surface topography in the mold manufacturing industry. In the future, the developed geometrical surface topography prediction software will be improved by considering the cutting mechanisms.

Key words: Machining simulation, surface topography, surface roughness, end mill, Korea

INTRODUCTION

Milling is a fundamental machining operation. End milling is the most common metal removal process. It is used in a variety of issued manufacturing industries aerospace, automotive, precision molds and dies. In industry, manual polishing is replaced by a high-quality milling process. Precision milling technology can be used to create micro patterns or mirror surfaces. A well-milled surface plays an important role in improving mechanical properties such as fatigue strength and corrosion resistance. Surface roughness affects several functional properties of parts such as surface friction, wear, heat transmission, light reflection, lubricating and distribution ability, coating and fatigue resistance.

Surface quality is affected by milling conditions and cutting mechanisms. Milling conditions consist of the feed, spindle speed, step over, tool geometry and slope angle. Static cutting mechanisms are tool wear, runout, backlash and heat. Dynamic cutting mechanisms are vibration, chatter, dynamic cutting force and machine control.

Surface quality prediction techniques are required to evaluate appropriate input parameters such as feed, spindle speed, step over and tool angle. These can be used to achieve the required surface roughness or topography in industry. It is also important that the prediction technique be accurate, reliable, low-cost and non-destructive. Prediction techniques are divided into statistical or geometric models. Amran *et al.* (2014) used the response surface method to estimate drill surface roughness. Babur proposed the development of a statistical model to estimate surface roughness in a high-speed flat end milling process under wet cutting conditions, using machining variables such as spindle speed, feed rate, depth of cut and step over (Ozcelik and Bayramoglu, 2006). Brito *et al.* (2014) proposed the normal boundary intersection method coupled with mean-squared error functions. This is an improvement over the statistical method. Corral *et al.* (2012) proposed a method that predicts topography and surface roughness in ball end milling processes, based on geometric tool-workpiece intersections. This allows the determination of surface topography as a function of feed per tooth and revolution, radial depth of cut, axial depth of cut, number of teeth, tool teeth radial, helix angle, eccentricity and phase angle between teeth. Tae-sung proposed a method to predict machined surface roughness in ball end milling (Jung *et al.*, 2004, 2005). This was named the “Ridge method” and deals with geometrical surface roughness in ball end milling. There have been laboratory level studies carried out that predict surface topography but this has not been achieved at an industrial level.

Therefore, the purpose of this study is to develop surface quality simulation software that predict surface roughness from the tool geometry and cutting conditions of the manufacturing industry.

MATERIALS AND METHODS

Prediction software

Development of prediction software: The tooth of an end mill rotates and translates during the milling process as shown in Fig. 1. The cutting speed of the centre of the

Corresponding Author: Su-Jin Kim, Department of Mechanical Engineering, Gyeongsang National University, 52818 Jinju, Republic of Korea

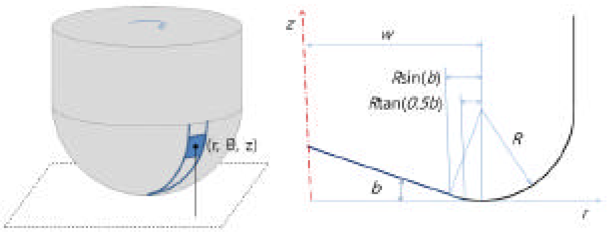

Fig. 1: Updating the z-buffer using the facet element of the generalized end mill geometry

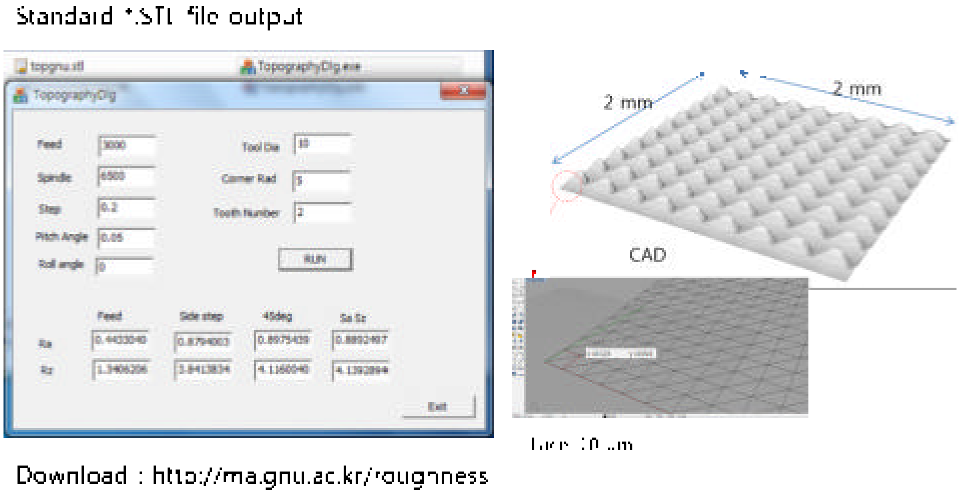

Feed 3000
Spindle 6500
Step 0.2
Pitch Angle 0.05
Roll angle 0
Tool Dia 10
Corner Rad 5
Tooth Number 2

	Feed	Side step	45deg	Sa Sz
Ra	0.4433040	0.8794003	0.8975439	0.8892407
Rz	1.3406206	3.8413834	4.1160040	4.1392884

Fig. 2: Micro surface topography prediction software

corner radius, R, affect micro surface topograph:end mill is zero and it increases as the radius increases. The trajectory of the tooth near the centre tip of the end mill is trochoid. The trochoid trajectory of the tooth is shown in Eq. 1. The first vector is the trochoid trajectory; the second matrix is the rotation of the tool and the final vector is which the translation motion of the tool:

$$\begin{bmatrix} x \\ y \\ z \end{bmatrix} = \begin{bmatrix} r\cos(\theta - n\pi) \\ r\sin(\theta - n\pi) \end{bmatrix} + \frac{\theta}{\pi}\begin{bmatrix} f_{t,x} \\ f_{t,y} \\ f_{t,z} \end{bmatrix} \tag{1}$$

Where:

x, y, z = Trochoid trajectory
θ = Rotation angle of tool
r = Radius on tool coordinate
n = Number of teeth
z(r) = Tooth curve on tool coordinate
ft = Feed per tooth

The tooth curve of the generalized end mill is expressed by Eq. 2. The bottom relief angle, b and tool

$$\begin{cases} z(r) = \{(w - R\tan(0.5b)) - r\}\tan(b), \text{if } r < w - R\sin \\ z(r) = R - \sqrt{R^2 - (r-w)^2} \text{ if } w - R\sin(b) < r < 0.50D \end{cases} \tag{2}$$

Where:

D = Tool diameter
R = Tool corner radius
w = Tool flat bottom rad (= 0.5 D-R)
b = Tool bottom relief angle

The workpiece is expressed by a z-buffer. The trochoid trajectory is divided into element facets. The intersection of the element facet and the z-buffer is calculated. If the z height of the buffer is higher than the intersection point, it is changed to the z height of the intersection point. The operation is repeated along the feed direction and side step direction of the tool path to obtain the machined surface topography.

The surface topography prediction software was developed using the Visual C++ language as shown in Fig. 2. The tool diameter, corner radius and tooth number are input to define the tool geometry. The feed, spindle speed and sidestep are input as the cutting conditions.

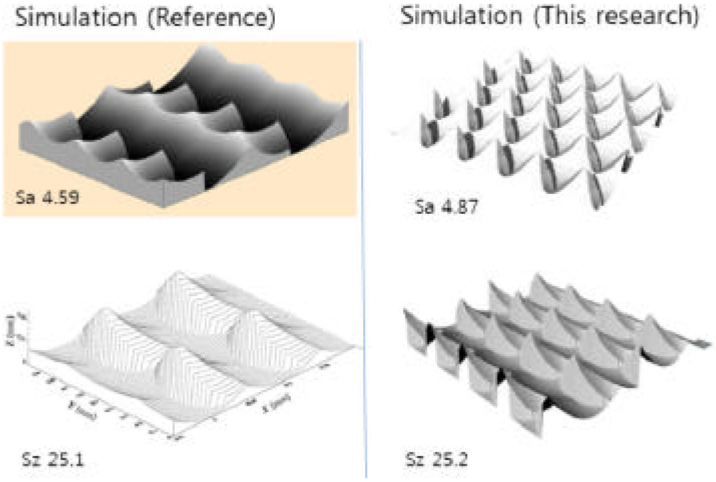

Fig. 3: Simulation surface topography of references and the developed software (Corral *et al*., 2012; Jung *et al*., 2005)

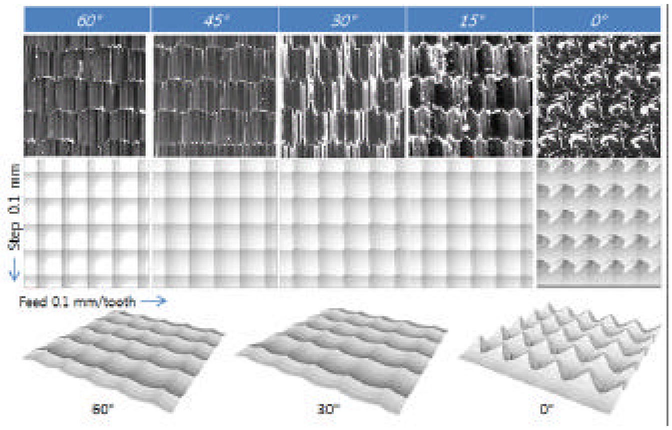

Fig. 4: Measured and simulated surface topography of inclined surfaces milled by a ball end mill

The pitch angle and roll angle are input to define the surface inclination of the workpiece. The software simulates micro machining of a 2×2-mm small workpiece. It outputs the micro surface in a standard STL file format all CAD software can read. The STL file expresses the surface in 10 μm sized triangles. The computation time was 9 sec. The complexity of the computation algorithm is O(n2). If the triangle size is decreased to 1 μm, the computation time is 430 sec on a personal computer with a 2.67 GHz CPU. The surface topography prediction software is opened from the website http://ma.gnu.ac.kr/roughness. All manufacturing industries are able to use the free software to predict machined surface topography and roughness.

Verification of the software: The developed software was verified by comparing with previous research results as shown in Fig. 3. The predicted surface of Iren is similar to this research when the diameter of the ball end mill, sidestep and feed per tooth are 6, 0.4 mm and 0.4 mm/tooth, respectively (Corral *et al*., 2012). The average areal roughness of Iren is 4.59 μm and that of this software is 4.87 μm. The predicted surface of Jung *et al*. (2005) is the same as this software when the diameter of the ball end mill, side step and feed per tooth are 10, 0.5 mm and 0.5 mm/tooth, respectively. The maximum arial surface roughness of Jung is 25.1 μm and that of the developed software is 25.2 μm. The verification results show that the developed software's machined surface predictions are similar to previous research.

The measured surface machined by a ball end mill is compared with the predicted surface in Fig 4. The diameter of the ball end mill is 3 mm and the

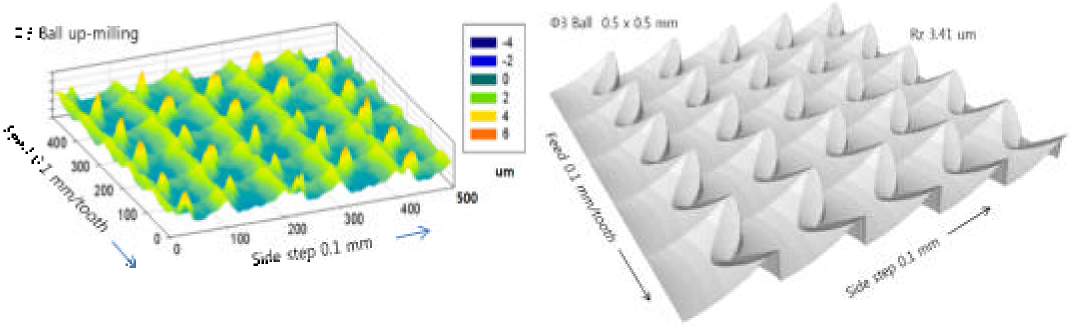

Fig. 5: Measured and predicted surfaces of the ball end mill

workpiece is made from STAVAX (HRC50). The feed per tooth, spindle speed and side step are 0.1 mm/tooth, 25000 rpm and 0.1 mm, respectively. The slope angle is changed to 60°, 45°, 30°, 15° and 0°. The micro surface machined by the side of the ball end mill is a pattern removed by a sphere in the feed per tooth and side step interval. The pattern is different to the others when the centre of the ball end mill cuts the work piece at 0°.

The surface topography of measured and simulated surfaces is shown in Fig. 5. It can be seen that the spatial wavelength of the measured and predicted surfaces is 100 μm. The height of the measured surface is approximately 4 μm is slightly bigger than the predicted height of 3.41 μm.

RESULTS AND DISCUSSION

Surface topography measurement: A stylus instrument is used to measure the surface roughness in a machine shop. A scanning electron microscope which was used to obtain images of the machined surface. Scanning white light interferometry (coherence scanning interferometry) was used to measure the machined surface topography in the laboratory. The full image section is obtained at the camera frame rate and height data are calculat whiched from interference information.

Surface topography of the ball end mill: The measured and predicted surfaces machined by a ball end mill are compared. The diameter of the coated carbide tool is 10mm. The workpiece is made from SM45C carbon steel. The spindle speed is 2900 rpm and side step is 0.2 mm. The feed per tooth is changed to 0.05, 0.1 and 0.2 mm/tooth. scanning white light interferometry and the predicted surface are shown in Fig. 6. The average areal roughness of the simulation micro surface is 69% less than the measured one when feed per tooth is one fourth of the side step as shown in Fig. 6a. The difference decreases to 27% when feed per tooth is increased to the same level whichas the side comparisons between the measured data using step as shown in Fig. 6c. The peak valley roughness when feed per tooth is one fourth of the side step is too large because, it is affected by measurement noise.

A photograph of whichthe machined workpiece is shown in Fig. 7. The developed surface quality prediction software considered geometrical milling conditions such as feed rate, spindle speed, step over, tool geometry and slope angle. However, it didn't consider the cutting mechanics that also affect surface quality. Static cutting mechanisms are tool wear, runout, backlash and heat. Dynamic cutting mechanisms are vibration, chatter, dynamic cutting force and machine control. The unconsidered cutting mechanics is the reason for big differences in the areal surface roughness between simulated and experimental results.

This study suggests a linear compensation method whichfor the predicted geometrical surface to the real surface that is affected by cutting mechanics. The linear compensation equation that minimizes the difference between measured and predicted data is written as follows:

$$S_{ac} = 0.55S_{as} + 0.64 \tag{3}$$

The peak to valley areal roughness is derived by multiplying the compensation constants of the average a real roughness by Eq. 4:

$$S_{tc} = 4\left(0.55S_{ts} + 0.64\right) \tag{4}$$

Figure 8 and Table 1, compare the differences between the experimental, simulated and compensated areal roughness. The average areal roughness error decreased from 69-1.1% after compensation. The peak to valley areal roughness error decreased from 75-11% after compensation.

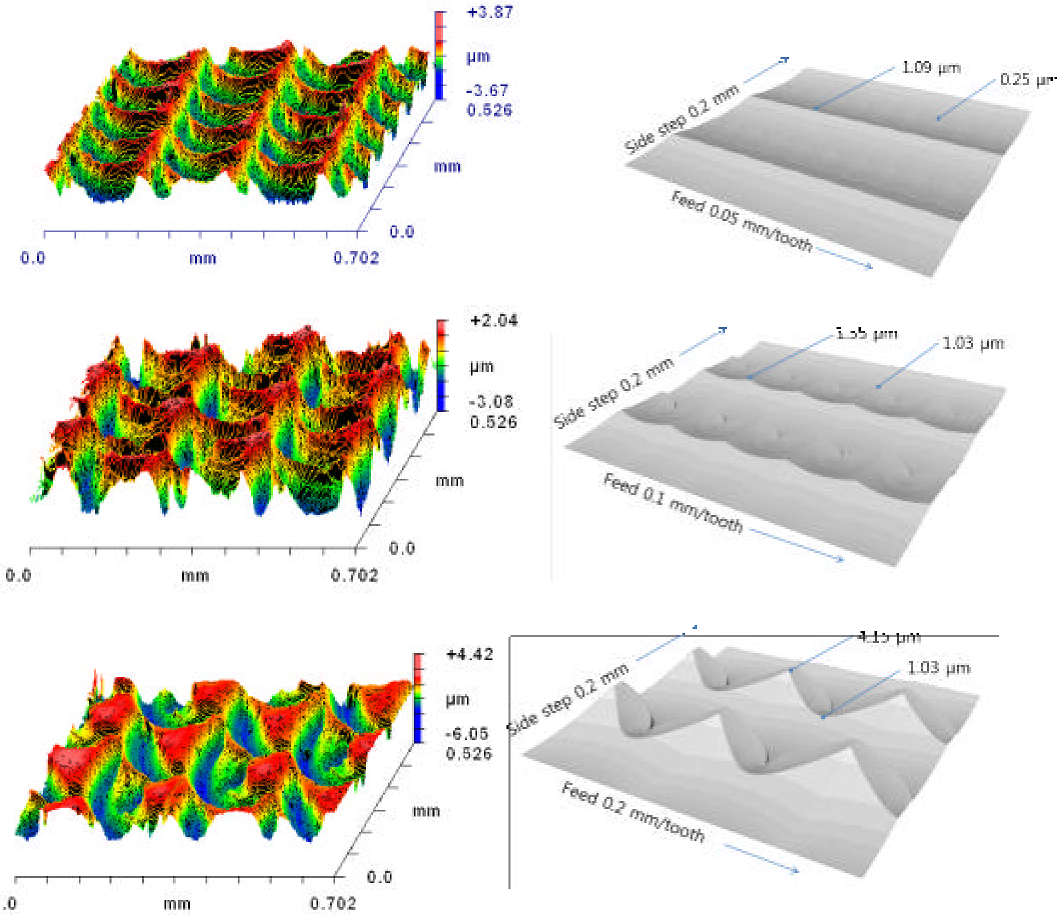

Fig. 6: Experimental and simulated surfaces of the ball end mill: a) Feed of 0.05 mm/tooth; b) Feed of 0.1 mm/tooth; c) Feed of 0.2 mm/tooth

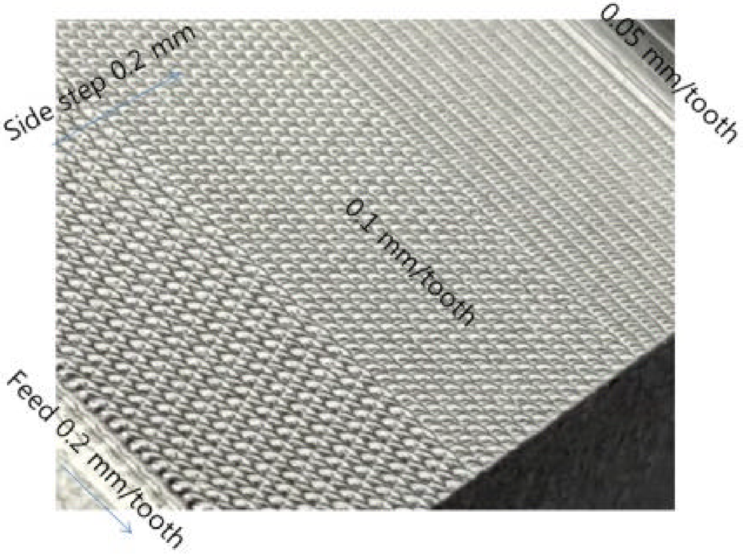

Fig. 7: Surface machined with a ball end mill

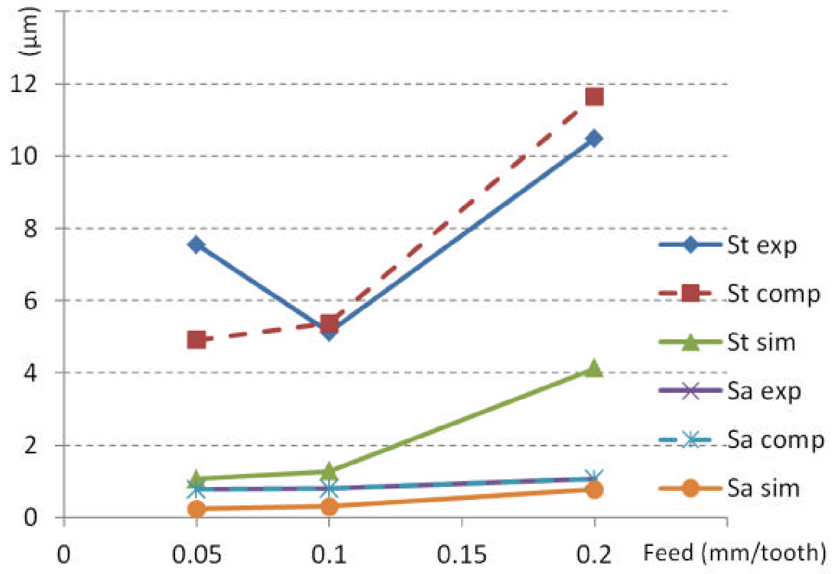

Fig. 8: Comparison of the experimental, simulated and compensated areal roughness of the ball end mill

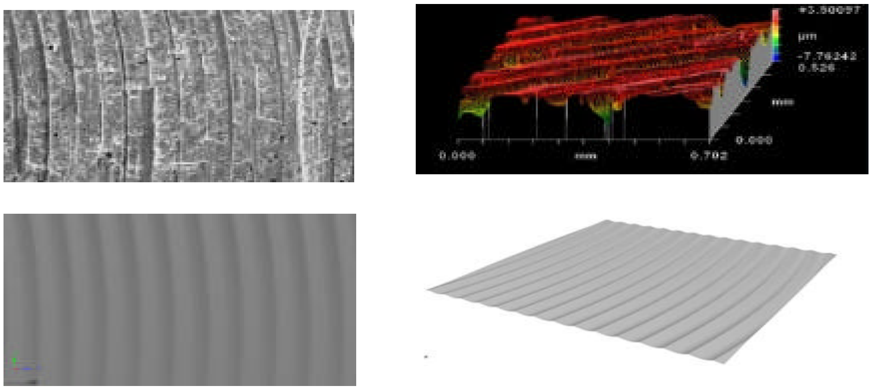

Fig. 9: Experimental and simulated surfaces of the flat end mill: a) Experimental; b) Simulated

Table 1: Comparison of experimental, simulated and compensated areal roughness

Variables	Feed (mmt^{-1})	Exp. (Mm)	Sim. (Mm)	Comp. (µm)*	Er_Sim. (%)	Er_Comp. (%)
S$_a$	0.05	0.78	0.24	0.77	69.2	1.1
	0.10	0.80	0.30	0.81	62.5	0.6
	0.20	1.07	0.78	1.07	27.1	0.1
S$_t$	0.05	(7.55)	1.07	4.91	(85.8)	(34.9)
	0.10	5.13	1.28	5.38	75.0	4.8
	0.20	10.48	4.13	11.65	60.6	11.1

() is affected by large measurement noise

Surface topography of the flat end mill: A comparison of the experimental results with the simulation data is shown in Fig. 9. The diameter of the tool is 10 mm and the corner radius is 1.0 mm. The tool is made from TiAlN-coated carbide produced by YG1 and the workpiece is made from SM45C carbon steel. The cutting feed is 500 mm min^{-1} (0.086 mm/tooth) and spindle speed is 2900 rpm. The arc pattern, with a radius of 5 mm, is shown in the top view of the experimental and simulated surfaces. The spatial wavelength of the experimental surface is 81 µm and the simulation result is 86 µm. The predicted height of the simulated surface is much smaller than the experimental surface measured by scanning white light interferometry. However, the surface roughness of the flat end mill was

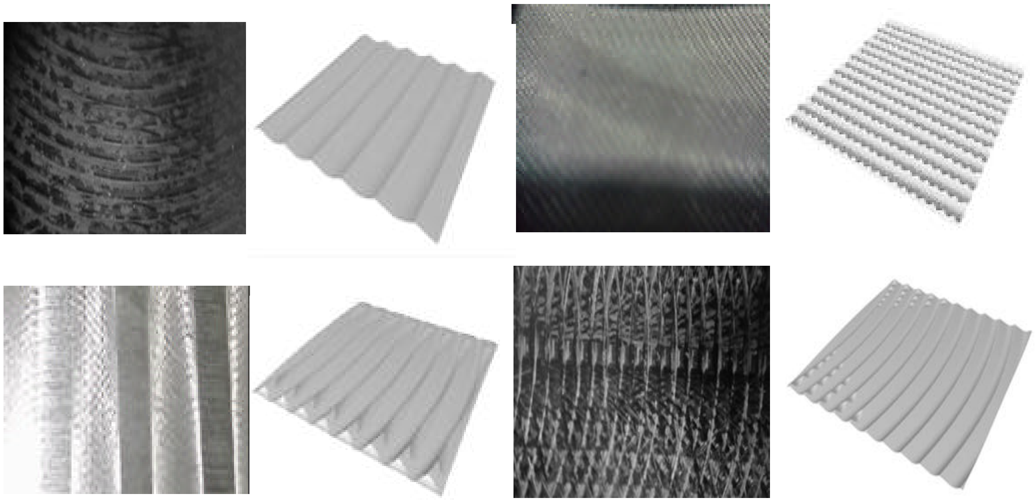

Fig. 10: Comparison of the micro surface of the real mold and simulated surface: a) Mold Ra 0.32 μm, Simulated Ra 0.44 μm; b) Mold Ra 0.64 μm, simulated Ra 0.78 μm; c) Mold Ra 0.93 μm, simulated Ra 0.58 μm d) Mold Ra 0.50 μm, simulated Ra 0.68 μm

too large because of dynamic tool deflection which could not be compensated by the linear compensation method suggested for the ball end mill.

Application software for the mold industry: The validated micro surface simulation software can be applied in the mold manufacturing industry. The image of the mold surface taken by the zoom lens of a camera is compared to the simulated surface as shown in Fig. 10. The surface patterns machined by the flat end mill and face cutter are shown in Fig. 10a-d. The arc patterns of the rotation tooth are shown in the real mold and simulation results. The surface patterns created by the ball end mill are shown in Fig. 10c. The average roughness measured by the stylus instrument is compared to the roughness calculated from the simulated surface. In the mold manufacturing industry, the difference between the measured roughness and simulation result has a maximum allowable value of 38%. The developed software is limited to geometrical surface topography in terms of the cutting mechanism which will be studied in future research. Tool wear (Safari and Izman, 2014), runout (Schmitz *et al*., 2007), tool deflection and chatter (Siebrecht *et al*., 2015) will be considered to improve the precision of the simulation results.

CONCLUSION

This study presents the development of software to predict the micro surface topography generated by an end mill. The software was developed using the Visual C++ language. Milling experiments and other previous research results were used to validate the estimation capability of the software.

The SM45C carbon steel was machined with a TiAlN-coated carbide end mill. The measured results were compared to the simulated results. A good agreement was found between reference data and prediction results. Furthermore, discrepancies between experimental and prediction results were compensated by linear equations and were assumed to be a consequence of different cutting mechanisms.

Finally, the validated micro surface topography software can be used to predict surface topography in the mold manufacturing industry. The real surface pattern of the mold was similar to which the simulated surface topography.

This research contributed to improving the laboratory level surface topography research to an industrial level by developing software and comparing results with real molds from industry.

In the future, the developed geometrical surface topography prediction software will be improved by considering the cutting mechanisms.

ACKNOWLEDGEMENT

We are grateful to the Ministry of Trade, Industry and Energy, who supported our research (No. 10048555).

REFERENCES

Amran, M., S. Salmah, M. Sanusi, M. Yuhazri and N. Mohamad et al., 2014. Surface roughness optimization in drilling process using Response Surface Method (RSM). J. Teknologi, 66: 29-35.

Brito, T.G., A.P. Paiva, J.R. Ferreira, J.H.F. Gomes and P.P. Balestrassi, 2014. A normal boundary intersection approach to multiresponse robust optimization of the surface roughness in end milling process with combined arrays. Precis. Eng., 38: 628-638.

Corral, I.B., J.V. Calvet and D.A. Fernandez, 2012. Surface topography in ball-end milling processes as a function of feed per tooth and radial depth of cut. Intl. J. Mach. Tools Manuf., 53: 151-159.

Jung, T.S., M.Y. Yang and K.J. Lee, 2005. A new approach to analysing machined surfaces by ball-end milling, part I. Intl. J. Adv. Manuf. Technol., 25: 833-840.

Jung, T.S., S.H. Nam, J.H. Park and M.Y. Yang, 2004. Analysis of machined surfaces by ball-end milling using the ridge method. J. Korean Soc. Precis. Eng., 21: 51-60.

Ozcelik, B. and M. Bayramoglu, 2006. The statistical modeling of surface roughness in high-speed flat end milling. Int. J. Machine Tools Manufacture, 46: 1395-1402.

Safari, H. and S. Izman, 2014. Influence of cutting conditions on surface and sub-surface quality of high speed dry end milling Ti-6Al-4V. J. Teknologi, 67: 131-135.

Schmitz, T.L., J. Couey, E. Marsh, N. Mauntler and D. Hughes, 2007. Runout effects in milling: Surface finish, surface location error and stability. Int. J. Mach. Tools Manuf., 47: 841-851.

Siebrecht, T., P. Kersting, D. Biermann, S. Odendahl and J. Bergmann, 2015. Modeling of surface location errors in a multi-scale milling simulation system using a tool model based on triangle meshes. Procedia CIRP., 37: 188-192.